ORIGINAL RESEARCH ARTICLE

Spatial distributions of on- and off-responses determined with the multifocal ERG

Anderson R. Rodrigues · Manoel da Silva Filho ·
Luiz Carlos L. Silveira · Jan Kremers

Abstract We studied the contribution of retinal on- and off-mechanisms in the multifocal electroretinogram (mfERG) by measuring responses to sawtooth stimuli. Six healthy subjects participated in this study. Rapid-on and rapid-off sawtooth stimuli with a period of 427 ms were presented in a multifocal pattern composed of 19 hexagons. The stimuli were interleaved with a blank field of the mean luminance and chromaticity. On- and off-responses were added to extract response asymmetries. The amplitudes of on-, off-, and added-responses were determined for different eccentricities relative to a signal baseline that was defined as the average of the electrical level recorded in two different time windows in which no responses were present. Measurements were repeated with eight different stimulus stretch factors to account for changes in retinal cell density as a function of eccentricity. The amplitudes of all ERG components decreased with increasing eccentricity for all stretch factors. For stretch factors between 0 and 20, responses to the central and immediately adjacent hexagons were large in amplitude. For more peripheral hexagons, the responses were very small or absent. Three components were identified in the on-responses ($N20_{on}$, $P46_{on}$ and $N100_{on}$). In the off-responses, we found one positive ($P20_{off}$) and one negative ($N90_{off}$) component, whereas in the addition, three components ($N20_{add}$, $P46_{add}$ and $N100_{add}$) could be observed. The $N20_{on}$ and $P46_{on}$ amplitudes decreased less steeply with eccentricity than the $N100_{on}$ amplitude, whilst the $P20_{off}$ and $N90_{off}$ amplitudes exhibited a similar decrease with eccentricity. In the addition, the two negative components exhibited a similar decrease in amplitude as a function of eccentricity and decreased more steeply than the positive component. The number of stimulated cones and retinal ganglion cells was estimated from anatomical data and compared with the responses. The spatial properties of the amplitudes of $N20_{on}$, $P46_{on}$, $P20_{off}$, and $N90_{off}$ and $P46_{add}$ were similar to those of the stimulated cone numbers. The remaining components had spatial characteristics that resembled those of the retinal ganglion cells. It is proposed that the ERG asymmetries revealed in the summed responses have post-receptoral origins, some of them reflecting the activity of the ganglion cell population. The use of sawtooth stimuli provide, similar to the pattern ERG, a way to record the ERG asymmetries.

A. R. Rodrigues · J. Kremers (✉)
Department of Ophthalmology, University Hospital
Erlangen, Schwabachanlage 6, 91054 Erlangen, Germany
e-mail: jan.kremers@uk-erlangen.de

A. R. Rodrigues · M. da Silva Filho · L. C. L. Silveira
Instituto de Ciências Biológicas, Universidade Federal
do Pará, Belém, Pará, Brazil

L. C. L. Silveira
Núcleo de Medicina Tropical, Universidade Federal
do Pará, Belém, Pará, Brazil

Introduction

The ERG response depends on the spatial and temporal characteristics of the visual stimulus that elicits it and can reveal complex waveforms and several nonlinearities. Often ERG recordings are obtained using short duration flashed stimuli that evoke a complex waveform with several components. The reason for the complexity is that a pulsed stimulus contains a broad spectrum of temporal frequencies, and the system that is being probed has a group of elements with different pulse response functions. In other words, in the ERG multiple components originate from different cell types that use different mechanisms to generate the recorded electrical activity. Other commonly used stimuli to obtain ERG recordings are temporal periodic stimuli for flicker ERGs or periodic reversals of spatial stimuli (gratings or checkerboards) for pattern ERGs, both responses being quite different from, and providing a range of additional information to, the flash ERG.

The disadvantage of brief flash ERGs is that the time between the on- and off-phases in the stimulus is so small that the responses to the luminance increase (the "on-response") and to the decrease in luminance (the "off-response") merge, and thus cannot be distinguished [1, 2]. To be able to distinguish between the on- and off-responses, either long-duration flash or ramped stimuli can be used. In the long flash ERG, [1, 2] the time between the onset and the termination of the light stimulus is large enough to disentangle the on- and off-responses. In contrast, ramps consist of a sudden luminance change (either rapid-on or rapid-off) followed by a relatively slow linear luminance increase or decrease. Because the ERG response to the slow phase is generally small at low temporal frequencies, these stimuli are suitable to isolate either on- or off-responses using rapid-on and rapid-off stimuli, respectively [3–6].

Similarly to long-duration flash stimuli [2, 7], the on- and off-responses obtained with sawtooth stimuli are quite dissimilar, and they seemingly bear hardly any relationship with each other [2, 3, 7]. The on-response shows an initial trough followed by a positive deflection, that is the homologue to the *b*-wave in the flash ERG and by a second trough that has about the same latency as the photopic negative response (PhNR) of the flash ERG. The off-response often only shows a marked positive deflection, the *d*-wave, followed again by a PhNR. The differences between on- and off-responses may originate in the response differences in the on- and off-retinogeniculate pathways once the polarities of the depolarizing and hyperpolarizing bipolar cell responses are reversed and are summed in the ERG [8]. Thus, the responses of depolarizing and hyperpolarizing bipolar cells are not simply mirror images of each other. The *b*-wave seems to originate mainly in depolarizing bipolar cells. Activity of the hyperpolarizing bipolar cells has a different influence on the ERG response [9], indicating an asymmetry in the ERG signals per se. In addition, on- and off-retino-geniculate pathways respond to both luminance increases and decreases. Similarly, the ERG responses to luminance increases and decreases do not necessarily isolate on- and off-mechanisms in the pathways leading to an ERG signal. However, they may reflect an asymmetry between the two, originating in nonlinearities in the mechanisms leading to the ERG response.

In several studies, these stimuli have been used to detect selective changes in the different components of the on- and off-responses caused by a retinal disorder [3, 4, 6, 10]. Furthermore, the spatial distribution of on- and off-responses was studied using a multifocal presentation [11, 12]. However, only few studies have concentrated upon a direct comparison between on- and off-responses, for instance, by looking at symmetries and asymmetries in the different components [7, 13, 14]. In the current paper, we present results of measurements with multifocal sawtooth stimuli to compare the on- and off-responses quantitatively. The asymmetry between the on- and off-responses can be extracted by adding the two. This asymmetry is probably also the cause for the pattern ERG with constant time and space average luminance: the responses to luminance increases in half of the checks are counteracted by the symmetrical responses to the luminance decreases elicited by the other half of the checks. The origin of the remaining response lies in the differences (the asymmetries) between the on- and off-responses [15]. The addition of responses to spatially homogeneous luminance

increases and decreases therefore can be expected to reveal the same response differences as the pattern ERG. Indeed, Viswanathan et al. [7] added the responses to the luminance increases and decreases in long flashes in anaesthetized monkey to simulate the pattern ERG. Related findings have been demonstrated in the human ERG first by Spekreijse's group [13, 14] and, more recently, by Simpson and Viswanathan [16]. Similarly, the responses to rapid-on and rapid-off sawtooth stimuli can be added to reveal the asymmetries that probably have inner retinal origins. But different from PERG, the sawtooth responses are less sensitive to optical blur. Thus, the method may be a useful alternative for the PERG under suboptimal optical conditions. It should be noted that by using small hexagons, optical blur may alter the size and contrast of retinal image of multifocal sawtooth stimuli as the ones used in this work. When exclusively due to the defocus, this effect could be compensated with appropriate refractive correction. Other compensatory strategies could be used for the decrease in contrast that may occur in other conditions such as cataract and certain forms of uveitis.

The retinal response to a patterned stimulus is influenced by the spatial properties of the stimulus since the different retinal cell types have distinct spatial distributions. For instance, the density of retinal ganglion cells decreases more steeply as a function of retinal eccentricity in comparison with the density of photoreceptors. It, therefore, can be expected that ERG responses originating from different retinal cell types will also have distinct spatial distributions. We have compared the spatial distribution of the different on- and off-response components using a multifocal presentation that varies in spatial scale, and we correlate the response asymmetries of these components density of cones and the retinal ganglion cells as a function of eccentricity to yield additional evidence about the cellular origins of these components.

Methods

Subjects

The study was performed in accordance with the tenets of the declaration of Helsinki. Six normal healthy subjects participated in this study (one 22-year-old female and five males between 27 and 32 years old). Five subjects had normal trichromatic colour vision. One subject was deuteranopic congenital colour blind. No difference was observed between the results obtained with the trichromatic and dichromatic subjects. Two subjects were 1.5 D myopic. None of them suffered from a retinal disorder. Informed consent was given by all subjects.

Visual stimulation

Multifocal ERGs using pseudorandom m-sequences were recorded with a VERIS Science 4.9 system (EDI, San Mateo, CA, USA). A 21" monochrome monitor (Nortech, Plymouth, MN, USA) with a 75 Hz refresh rate was used to present multifocal stimuli composed of 19 hexagons. Stimulus size was kept constant throughout the experiment: 315 mm × 291 mm or 51° × 47.6° at the view distance of 330 mm. The luminance of each individual hexagon was changed during one phase of the m-sequence according to a sawtooth function with a period of 427 ms. The luminance change was accomplished in 32 sequential frames of the monitor. A graphical presentation of an m-phase can be found in Fig. 1. Two different presentations were used: for rapid-on stimuli, a linear decrease from the mean luminance of 98.7 cd/m^2 to about 0.34 cd/m^2 was followed by an abrupt increment to a maximum level 187.5 cd/m^2. This sudden luminance change occurred in the middle of an m-sequence phase (from frame 16 to 17). After the sudden change, the luminance decreased linearly to the mean luminance. The rapid-off stimuli consisted of linear increase from mean luminance to a level of 187.5 cd/m^2 followed by the rapid change to 0.34 cd/m^2, and by a linear increase back to the mean luminance. In each hexagon, either the sawtooth stimulus or a blank period of 427 ms was presented (98.7 cd/m^2, $x = 0.3321$, $y = 0.3500$). Monitor luminance and chromaticity were measured using a LS-100 Photometer (Konica Minolta, Mahwah, NJ, USA) and a CAS 140 Spectrometer (Instrument Systems GmbH, Munich, Germany), respectively. It should be noted that at each phosphor location in a CRT display, a brief intense pulse is displayed at the beginning of its video frame, and therefore, the ramps are not linear increases or decreases in luminance but were generated in 16 discrete luminance steps with fast decays. Thus, Fig. 1 is an idealization of the actual luminance
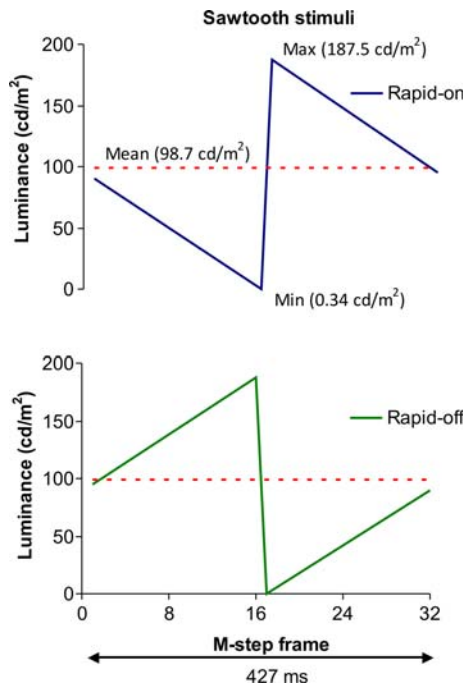
Fig. 1 Sketch of the sawteeth stimuli used to elicit ERG multifocal responses. The *plots* represent the luminance change of an *m*-step in each hexagon of the visual stimulus. For rapid-on sawtooth (*top*), there was an abrupt luminance increment to 187.5 cd/m^2 followed by a linear luminance decrease. For rapid-off sawtooth (*bottom*) there was an abrupt decrement to 0.34 cd/m^2 followed by a linear luminance increase. The sawtooth waveform period lasted 32 frames at a frame rate of 75 Hz (i.e. 427 ms corresponding to a temporal frequency of 2.34 Hz). For each stimulus hexagon element, a pseudorandom *m*-sequence determined the succession of either a sawtooth modulation or mean luminance stable presentation

changes during stimulus presentation taking into account the temporal resolution of visual system.

The responses to the two ramp stimuli were measured in separate sessions. Each ramp recording lasted approximately 14 min (*m*-sequence exponent = 11), which was divided into 4 equal segments. For every subject, measurements were repeated with eight different stretch factors (0, 1, 2, 10, 20, 30, 40, and 50) that changed the stimulus spatial conformation. We used different stretch factors because we wanted to obtain hexagon midpoints at different retinal eccentricities. Moreover, with larger stretch factors, we were able to get measurable responses at larger eccentricities because the eccentric hexagons were larger. With the small stretch factors, the signal-to-noise ratio was particularly large for the central responses. When the stretch factor was increased, the size of the central
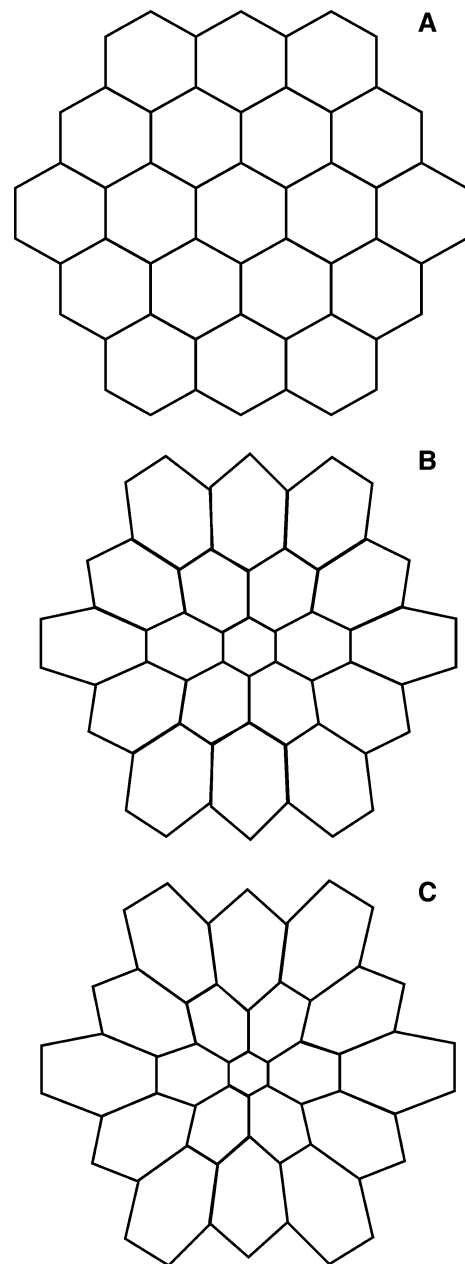
Fig. 2 Three spatial arrangement of the stimuli in the mfERG experiments for stretch factor values: 0 (**a**), 20 (**b**) and 50 (**c**). Stimuli comprised 19 hexagons whose size and shape changed accordingly to eight different stretch factor values. With increasing stretch factor, the size of the central hexagon decreased, whereas the more peripheral hexagons became larger and stretched in the radial direction

hexagon decreased, whereas the more peripheral hexagons became progressively larger and stretched in the radial direction (see Fig. 2 for examples).

Procedure

The subjects were seated in front of the stimulus monitor and rested their heads on a chin rest with the eyes 33 cm from the screen. Subjects were asked to fixate on a cross in the middle of the screen. ERGs were recorded from the right eye using DTL electrodes. Gold cup electrodes placed on the ipsilateral temple and the forehead were used as reference and ground electrodes, respectively. Of each subject, the pupil of the right eye was dilated by a drop of Tropicamide (Mydriaticum, Stulln Pharma, Germany). The use of Tropicamide paralyses accommodation and may alter the size of the retinal images of the different hexagons differently for subjects with different refractive errors. However, as the range of refractive errors was small (four subjects were emmetropic and two 1.5 D myopic), we decided to avoid refractive correction. If requested, a topical anaesthetic (Oxybuprocain; Alcon Pharma GmbH, Freiburg, Germany) was administered. The signals were amplified 100,000 times, and bandpass filtered with 3 and 100 Hz cut-off frequencies by a Grass Neurodata Acquisition System Amplifier Model 12 (Grass Instruments, W. Warwick, RI, USA). The left eye was covered by an eye patch during the recordings.

Data analysis

The ERG response may reveal several nonlinearities that may affect all subsequent retinal processes. It is expected that ERG components will have more nonlinearities if their origins are located in the inner retina when compared with those components that originate in the photoreceptors, or in other cells of the outer retina, because nonlinearities tend to be cumulative. One of the properties of linear processes and simple contrast dependent nonlinearities is that the response to a sign inverted stimulus is also sign inverted. This fact is derived for linear systems from the property of the additivity or superposition principles, which state that the response to an addition of two stimuli equals the sum of the responses to each separate stimulus:

$$R(S_1 + S_2) = R(S_1) + R(S_2)$$

As a consequence, the responses to a stimulus and its inverse cancel out when they are added:

$$R(S_1) + R(-S_1) = R(0) = 0$$

Thus, when the responses to the two sawtooth stimuli are added, linear responses and possibly simple contrast dependent nonlinearities cancel each other out, and asymmetrical nonlinearities in the ERG response, which most probably originate at a post-receptoral level, will be revealed.

The mfERG responses to rapid-on and rapid-off stimuli have components whose correspondence to the full-field flash ERG can be established on the basis of their sequences and latencies. The on-response contains an initial trough that is the homologue to the ERG a-wave, having a latency of about 20 ms after the rapid luminance change of the stimulus. This early negative wave is followed by a positive component, equivalent to the b-wave, which peaks between 40 and 50 ms after the rapid luminance change. Finally, there is a late negative wave with a minimum occurring between 80 and 160 ms. In the rapid-off response, the first positive component, equivalent to the full-field flash ERG d-wave, peaks between 15 and 70 ms, and it is followed by a negative component peaking between 80 and 160 ms. Whilst the positive waves can be compared to the b- and the d-waves, the late negative waves are homologous to the PhNR on and PhNR off that have been previously described in monkeys and humans.

A signal baseline was defined as the averaged potentials recorded in two different time windows, 0–15 ms and 160–182 ms. Within these intervals, we were confident that no recordable ERG responses were present. In addition, by averaging the signals within these two intervals assured a baseline estimation that was based on the largest possible fraction of the total recording time. In order to obtain an estimate of intrinsic noise, three different noise definitions were used, which corresponded to (1) the difference between the mean baseline level and to the most positive value in the windows ($P1_{noise}$); (2) the difference between baseline and the lowest value ($N1_{noise}$) and (3) the difference between the lowest and the highest value ($P2_{noise}$ which equals $P1_{noise} + N1_{noise}$). For all three noise definitions, the aforementioned two time windows were used. Three different noise values were estimated, because for each signal, we estimated a noise value using the same procedures as were used to measure the signals. This ensured the estimation of the signal-to-noise ratio.

The amplitudes of mfERG waveform components were measured as follows. For rapid-on responses, the $N20_{on}$ amplitude was defined as the difference between the baseline and the first trough from which the $N1_{noise}$ was subtracted; the amplitude of the $P46_{on}$ component was taken as the difference between the first trough and the first positive peak, corrected by the $P2_{noise}$ value; and the $N100_{on}$ amplitude was measured from the baseline to the second negative trough and corrected by $N1_{noise}$. For rapid-off responses, the $P20_{off}$ amplitude was defined by the difference between the baseline and the first positive peak, corrected by $P1_{noise}$; the $N90_{off}$ amplitude was estimated by the difference between the baseline level and the late negative trough from which $N1_{noise}$ is subtracted.

The time elapsed from stimulus onset to the peak of each of these components was taken as the component implicit time. The definitions of the different response components are also displayed in Fig. 3. Observe that the implicit times in this particular measurement may deviate somewhat from the averaged implicit times of each component used for the nomenclature (see also Fig. 11). The use of a nomenclature for the ERG components that has specific implicit times associated with it might be questionable. It is well known that ERG or VEP (visual evoked potential) components have implicit times (or latencies) that varies amongst individuals or even change with several stimulus parameters such as spatial frequency or contrast. However, it makes easier to follow experimental results keeping the ERG nomenclature obtained from an "average" individual at optimum stimulus condition.

Results

Figure 3a–b shows some examples of mfERG responses, recorded in the same subject, to rapid-on and rapid-off sawtooth stimuli for the central hexagon. A stretch factor 0 was used in this recording. The responses to rapid-on and rapid-off stimuli are quite different, and they are not mirror images of each other, indicating a large degree of asymmetry in the responses. Figure 3 also clearly displays that the positive components in the off-response and on-response ($P20_{off}$ and $P46_{on}$, respectively) have different implicit times, suggesting the involvement of
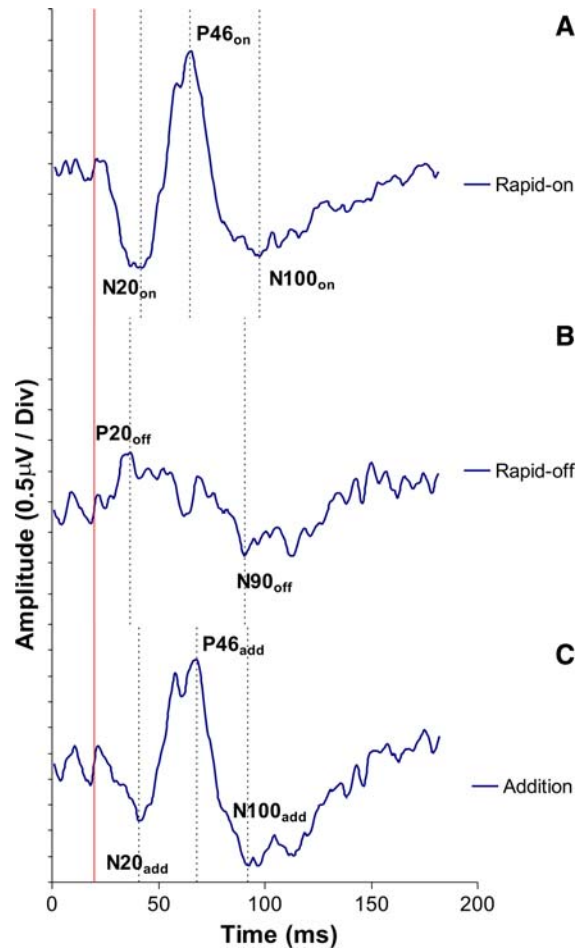
Fig. 3 Multifocal ERG responses for the central hexagon of the rapid-on (**a**) and rapid-off (**b**) sawteeth stimuli recorded from a single subject using the 0 stretch factor. The *peaks* of the early negative ($N20_{on}$), the positive ($P46_{on}$) and late negative ($N100_{on}$) components of the mfERG response elicited by rapid-on and early positive ($P20_{off}$) and late negative ($N90_{off}$) components of the mfERG response elicited by rapid-off stimuli are indicated by *vertical dotted lines* and labelled accordingly. Note that the nominal time of occurrence is only an approximation. The real latencies were measured. The *vertical red line* indicates the time of the rapid luminance change in the stimulus. **c** Waveform resulting from the addition of rapid-on and rapid-off responses. Their components are indicated and labelled similarly to the original responses

cellular processes with different temporal properties in these components. The timing of both the positive and negative responses following both light onset and offset, as well as in the averages (see below), is slightly delayed in comparison to the timing of similar components in the long flash ERG responses that have been previously published [2].

Figure 3c displays the waveform resulting from the addition of the rapid-on and the rapid-off responses. The summed response conserves the same main components observed in the rapid-on response, but important differences can be noted. First, the $N20_{on}$ amplitude is larger than the $N100_{on}$ amplitude, and the opposite is the case for $N20_{add}$ and $N100_{add}$. This indicates that in the addition procedure, $N20_{on}$ was partially cancelled by $P20_{off}$, suggesting that they have at least partially similar cellular origins and that they may reflect some degree of linearity. However, a substantial $N20_{add}$ response is present revealing that the cancellation is incomplete and some response asymmetry is present. This response resembles the N35 component of the pattern ERG.

To evaluate the spatial distribution of different components of the rapid-on, rapid-off and summed responses, we measured their amplitudes and latencies for the different retinal eccentricities. The response amplitudes to stimulus hexagons located at the same eccentricities were averaged. Figures 4, 5 and 6 display the means and standard deviations of response amplitudes of all subjects that were plotted as a function of retinal eccentricity of the hexagon midpoints. Observe that the locations of the hexagon midpoints are slightly different for different stretch factors. Furthermore, plotting the data as a function

of eccentricity is not identical as plotting them for separate rings, because the hexagons in ring 2 have not all identical eccentricities. In each figure, the results were plotted separately for different stretch factors. For small values of the stretch factor, between 0 and 20, significant responses to the central and immediately adjacent hexagons were obtained. For more eccentric hexagons, the responses were very small or absent. Comparison of Figs. 4 and 6 shows that at all eccentricities and for all stretch factors, the absolute $N20_{on}$ amplitude was larger than the $N100_{on}$ amplitude whilst the opposite is the case for $N20_{add}$ and $N100_{add}$ amplitudes, confirming the observations for the central hexagon responses displayed in Fig. 3 that the $N20_{on}$ is partially cancelled by the $P20_{off}$ component.

The amplitudes of all components decrease with increasing eccentricity for all stretch factors. To be able to compare the spatial distribution of the different components, the responses measured at eccentric locations were normalized to the response measured in the central hexagon (Figs. 7, 8 and 9). The areas under the curves of these normalized values were calculated and used as an index for the profile of the decrease in the different response components: a strong eccentricity dependent decrease results in small areas under the curve whilst a more


Fig. 4 Averaged rapid-on response amplitudes as a function of retinal eccentricity of the hexagon midpoints for different stretch factors (the results of four out of eight used stretch factors are shown in the different panels). The amplitudes of all three mfERG components decreased with eccentricity for all stretch conditions. At all eccentricities and for all stretch factors, $N20_{on}$ amplitudes were larger than $N100_{on}$ amplitudes
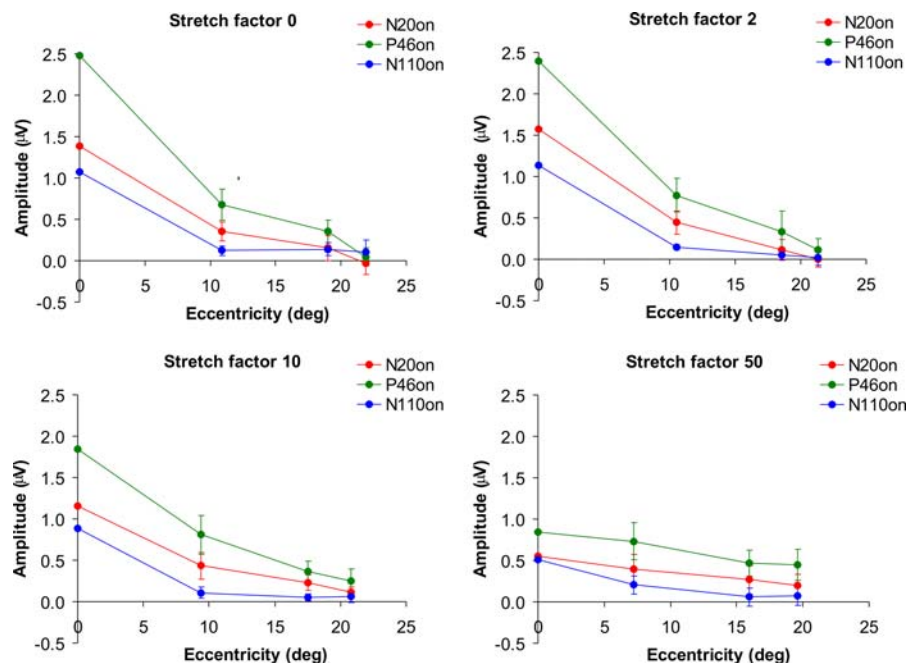
Fig. 5 Rapid-off response amplitude given as a function of eccentricity for different stretch conditions. The same format as for Fig. 4 was used. At all eccentricities and for all stretch factors, P20$_{off}$ amplitudes were larger than N90$_{off}$ amplitudes
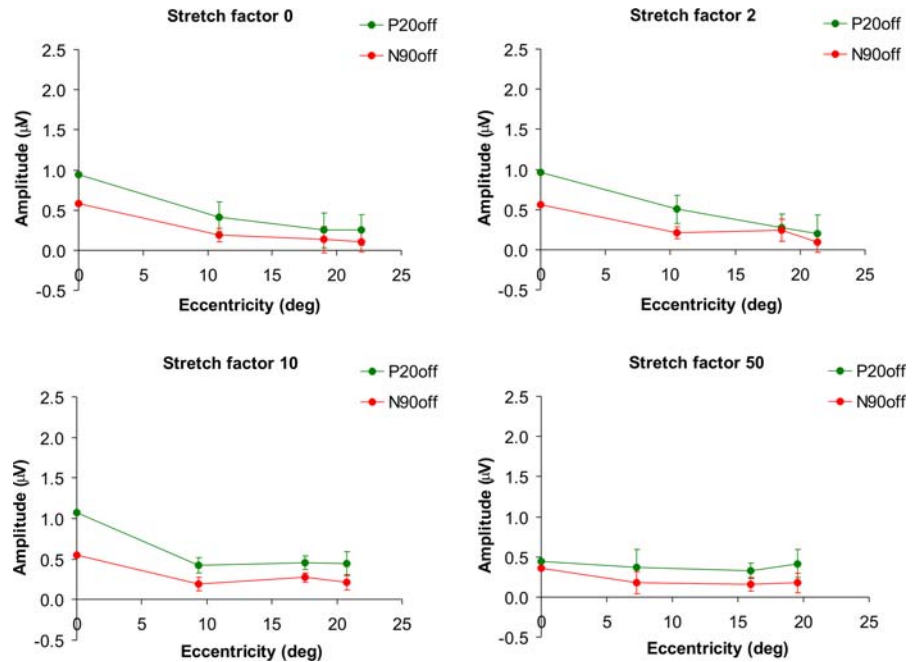
Fig. 6 Amplitude of the addition of rapid-on and rapid-off responses given as a function of eccentricity for different stretch conditions. The same format as for Figs. 4 and 5 were used. Differently from rapid-on responses (Fig. 3), N100$_{add}$ amplitudes were larger than N20$_{add}$ at all eccentricities and for all stretch factors
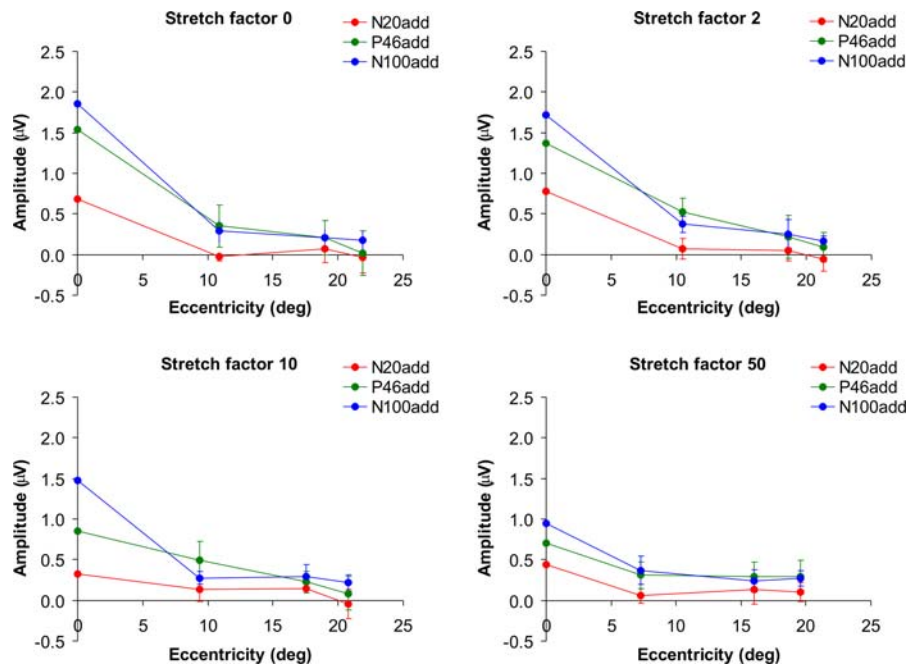
gradual decrease results in large areas. At stretch factor zero, N100$_{on}$ decreases more steeply than the other two on-response components. When the stretch factor is increased, the amplitudes of all components decrease less steeply with increasing eccentricity although this is not as obvious for the N100$_{on}$ as for

the other components. Both components of the off-response exhibit similar eccentricity dependent decreases for the zero stretch factor condition. The decrease is less pronounced when the stretch factor is increased but remains similar for both components. The difference between the N100$_{on}$ and the other two

Fig. 7 Relative amplitude of rapid-on response components as ▶ a function of visual field eccentricity for different stimulus stretch factors compared with the relative number of ganglion cells (GC) and cones (CC) that were presumably stimulated in each stimulus condition. The values are normalized to one in the central hexagon. For stretch factor equal to zero, the amplitude of the $N100_{on}$ component decreased more steeply with eccentricity than the amplitude of the other two components, $N20_{on}$ and $P46_{on}$. When the stretch factor was increased, the $N100_{on}$ amplitude decreased at about the same rate whilst the $N20_{on}$ and $P46_{on}$ amplitudes decreased less steeply with eccentricity. GC and CC numbers were estimated from available data in the literature for humans [19–21]. For each stretch factor, the central hexagon area and the area corresponding to hexagons located at a similar eccentricity were multiplied by GC and CC densities to estimate the number of cells. For small stretch factors (0–10), $P46_{on}$ and $N20_{on}$ amplitudes decreased with eccentricity at about the same rate as the number of cones, whilst $N100_{on}$ amplitude decreased with eccentricity following the decrease in the number of ganglion cells


components of the rapid-on response disappeared after the rapid-on and rapid-off responses were added.

To enable a comparison between response amplitudes and cell distribution, we estimated the numbers of stimulated cones and ganglion cells based on data from macaque monkey [17, 18] and humans [19–21], normalized to the numbers in the central hexagon. For the human retina, linear distance was converted to angular distance using wide angle schematic eye of Drasdo and Fowler [22]. For the ganglion cell density distribution in the human retina, two data sets were available. Curcio and Allen [20] counted ganglion cells across the entire retina but have not provided an estimate of ganglion cell sampling density in the central retina that could be directly compared with our ERG measurements. On the other hand, Sjöstrand and colleagues [21] presented a detailed estimate of the radial displacement of fibres of Henle, bipolar cells and ganglion cells and calculated how ganglion cell sampling density changes across the central 3 mm using their own counts and those of Curcio and Allen. Thus, we combined the two data sets to cover the range of eccentricities that we studied. The comparison between response amplitudes and cell distribution in the human and monkey retinae provided similar results, but only the comparisons with human retinal cell densities are plotted in Figs. 7, 8, 9 and 10. For small stretch factors, the amplitude decrease in the $N20_{on}$ and $P46_{on}$, $P20_{off}$,
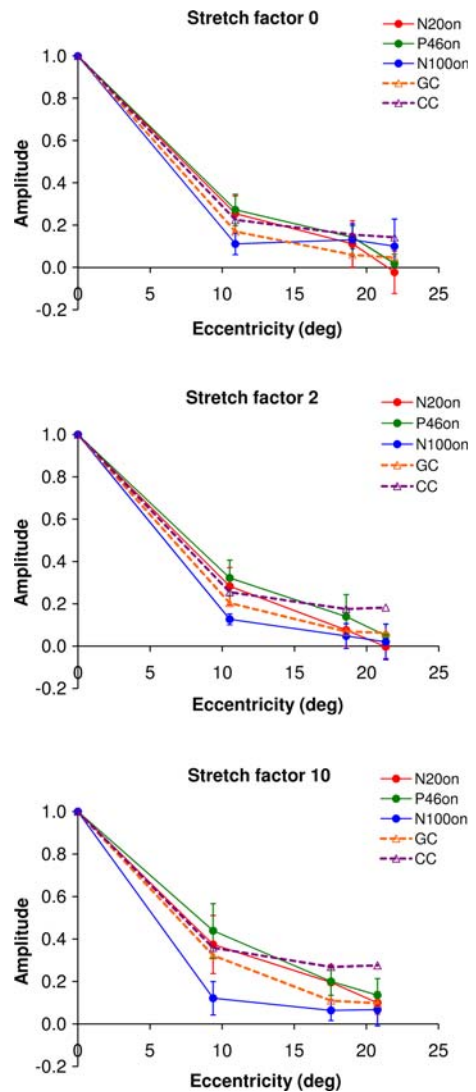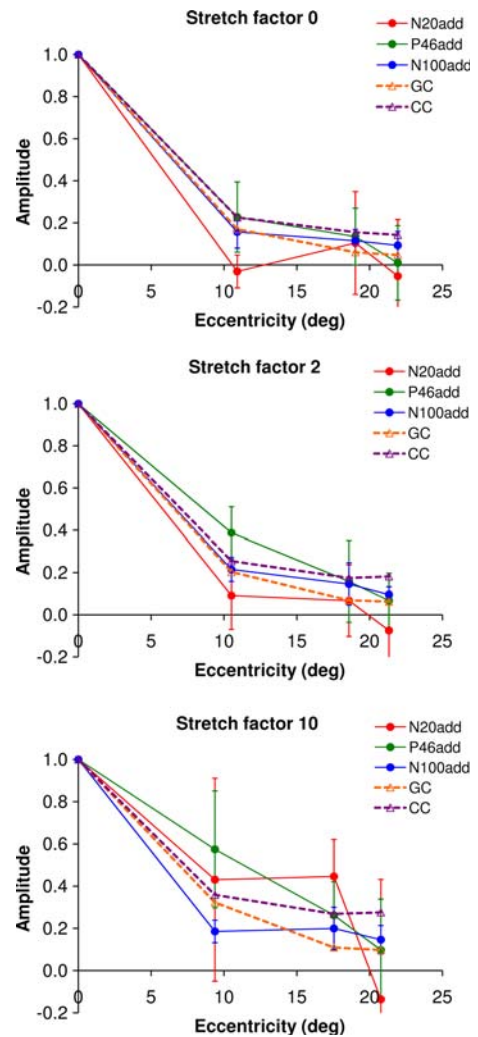
and $N90_{off}$ components follows the decrease in cone numbers, whereas for the $N100_{on}$ component, the decrease resembles that of the ganglion cell population. When the stretch factor is increased, the decrease in the $N20_{on}$ and $P46_{on}$ components became steeper than the decrease in the number of cones. In the added responses, a good correlation between $N100_{add}$ amplitude and number of ganglion cells was obtained for a wider range of stretch factors, whilst the other two components exhibit a less consistent correlation with either the number of cones or ganglion cells.

In Fig. 10, the area under the curves of the response components and the stimulated cell numbers
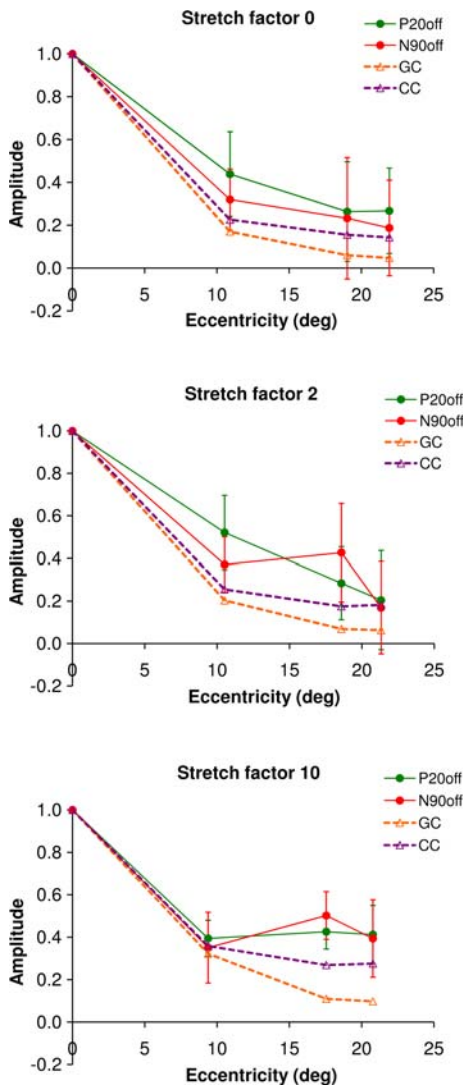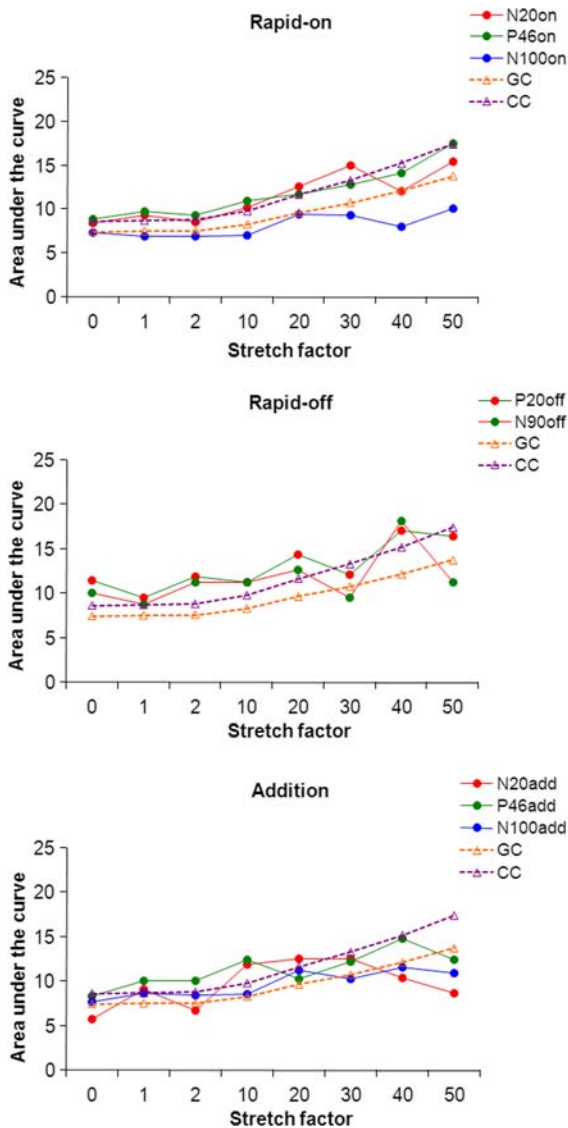
Fig. 8 Relative amplitude of rapid-off response as a function of eccentricity for different stimulus stretch factors together with the estimated relative number of ganglion cells (GC) and cones (CC) that were stimulated. Both components of the rapid-off response showed a decrease with that resembled the decrease in the number of stimulated cones

Fig. 9 Relative amplitude of added rapid-on and rapid-off response given as a function of visual eccentricity together with the relative number of stimulated ganglion cells and cones. The decrease in the $N100_{add}$ amplitude was similar as the decrease in the stimulated ganglion cells. There was no correlation between the rate of change of the $N20_{add}$ and $P46_{add}$ amplitude with the ganglion cell or cone counts along eccentricity

are displayed for the different stretch factors. Because the curves shown in Figs. 7, 8 and 9 decrease less steeply, the area under the curves increase when the stretch factor increases. More importantly, for small stretch factors, the area under the curves of the $N100_{on}$ and the negative components in the addition resemble those of the retinal ganglion cells, whereas those of the $N20_{on}$, the $P46_{on}$ the two off-components and the $P46_{add}$ are more similar to those of the cones.

For larger stretch factors (>10), the area under curves were generally smaller for the response components than for the cell numbers, indicating that the responses decreased more steeply with increasing eccentricity. Generally, a two-tail Spearman's correlation analysis showed a significant (95% confidence interval) correlation between the areas under the curve for the $N100_{on}$ and the $N100_{add}$, and the $N20_{add}$ and those of the retinal ganglion cell numbers (the

Fig. 10 Eccentricity dependent amplitude change of mfERG components, defined as the areas under the curves given in Figs. 7, 8 and 9 given for the different stretch factors. The continuous curves are the areas under the curves for the stimulated cones and retinal ganglion cells in the human retina, given as a function of retinal eccentricity

smaller than 0.4 when correlated with ganglion cell numbers).

Figure 11 shows the implicit times of different mfERG components in the on-responses as a function of retinal eccentricity of hexagon midpoints. These data are plotted separately for different stretch factors, and only responses that were above noise level were considered. When eccentricity is increased, the implicit times of all response components were generally constant with the exception of $N100_{on}$. The implicit times of this component tend to increase with increasing eccentricity. This was, to a lesser extent, also the case for the $N100_{add}$ component (data not shown). The implicit time of all other components were fairly constant at different eccentricities.

Discussion

The goal of the present study was to investigate the contributions of on- and off-retinal pathways to the mfERG signal, to determine asymmetries between the two and to find a possible correlation between the different mfERG components and receptoral and post-receptoral mechanisms.

Our results showed the $N20_{on}$ and the $P20_{off}$ components had complementary profiles, suggesting that they had similar cellular origins and that these responses were at least partially linear. The $N20_{on}$ component is probably the homologue of the *a*-wave in the flash ERG and originates in cone photoreceptor and off-bipolar cell activity [23, 24]. In addition, it is supposed that cone and off-bipolar cell activity can also contribute to the ERG *d*-wave component, which can be considered to be the homologue of the $P20_{off}$ component [25]. Our results were in agreement with these earlier data because we observed that these two components cancelled each other out to a large extent when the on- and off-responses were added, and this indeed suggests that they have similar origins and that these responses originate in the photoreceptors and outer retina. This is in agreement with the fact that the eccentricity dependent amplitude decrease and the amplitude under the curves follow the density profile for the cone photoreceptors.

The late negative component in the addition ($N100_{add}$) of on- and off-responses was larger than either $N100_{on}$ or $N90_{off}$. These components are most

values of the Spearman's correlations for these components were 0.905, 0.801 and 0.737, respectively; these components had Spearman's correlation values smaller than 0.8 when correlated with cone numbers), whereas all other components showed a closer correlation with the area under the curve for cone numbers (Spearman's correlation values larger than 0.85, whereas the correlations displayed values

Fig. 11 Average values for implicit times of mfERG components elicited by rapid-on stimuli at different eccentricities plotted separately for four different stretch factors. The $N100_{on}$ latency increased with increasing eccentricity whilst for $N20_{on}$ and $P46_{on}$, there was very little or no change. This trend was present for all stretch factors
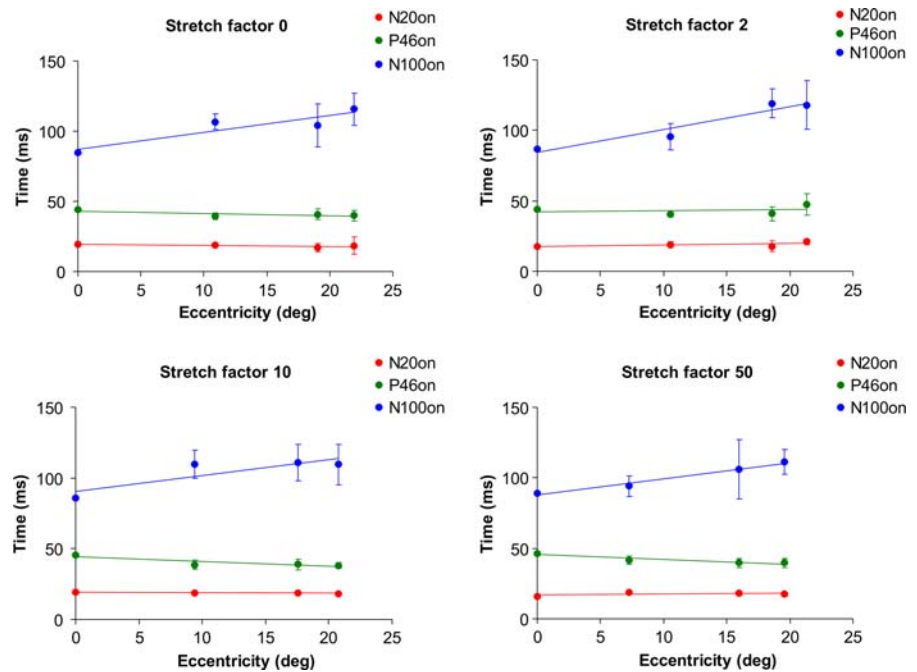
probably homologues to the photopic negative response (PhNR) of the flash ERG, which originates in the spike generating mechanisms of ganglion and amacrine cells [7, 26, 27]. The large asymmetry in the late negative components is agreement with this hypothesis, assuming that components with more proximal origins have generally stronger asymmetries.

As the addition of the on- and off-responses is possibly a simulation of the PERG [7], the $N100_{add}$ is also the homologue of the PERG N95 component. This is in agreement with data showing that this PERG component also originates in the retinal ganglion cells (see Holder [28] for a discussion on the origin of the PERG components). Our finding that the spatial properties of the response amplitudes of $N100_{add}$ resembled those of stimulated ganglion cells numbers is a further indication of the proximal origin of this component. The small but consistent difference between the implicit times of $N100_{on}$ and $N90_{off}$ suggests that these two components do not have identical origins. This notion is strengthened by the finding that the implicit time of the $N100_{on}$ increases with increasing retinal eccentricity, whereas the $N90_{off}$ implicit time does not change substantially with retinal eccentricity. Finally, unlike the $N100_{on}$ the $N90_{off}$ has spatial properties that resembled those

of the number stimulated cones rather that of the retinal ganglion cells.

Our results support previous findings of Kondo et al. [29], showing that the response densities for all mfERG components (a-, b-, and d-waves) decreased with increasing retinal eccentricities, the ratio of the d-wave to b-wave amplitudes was minimal in the central retina and increased towards the periphery and that the ratio of a-wave to b-wave amplitudes also increased towards the peripheral retina.

If the added responses are a simulation of the PERG, it can be expected that the response described in the present study is similar to multifocal PERG responses [30–32]. Data on normal subjects with the hexagon configuration as used in the present paper gave amplitude profiles similar to ours [30], although a quantitative comparison is not always straightforward because of differences in recording conditions. The direct comparison between ERGs evoked by multifocal sawtooth stimuli as used in this work and PERGs should, however, be made with caution because there are additional PERG contributions to consider, such as edge effects and lateral interactions including spatial tuning of response generators. In contrast with the PERG, the addition of on- and off-responses as performed in this work is less sensitive

to optical factors. Although we have not directly tested this issue, the measurement of response asymmetries to rapid-on and rapid-off sawtooth stimuli may be a useful alternative in conditions in which the optical conditions prohibit the measurement of a PERG. Our measurements were performed using multifocal stimuli made of hexagons with sharp borders and so the responses may be sensitive to optical blur to a certain extent. However, it can be predicted that by adding on- and off-responses to full-field stimuli as a simulation of the PERG, this problem can be overcome.

References

1. Sieving PA (1993) Photopic on- and off-pathway abnormalities in retinal dystrophies. Trans Am Ophthalmol Soc 91:701–773
2. Sustar M, Hawlina M, Brecelj J (2006) ON- and OFF-response of the photopic electroretinogram in relation to stimulus characteristics. Doc Ophthalmol 113:43–52
3. Alexander KR, Fishman GA, Barnes CS, Grover S (2001) ON-response deficit in the electroretinogram of the cone system in X-linked retinoschisis. Invest Ophthalmol Vis Sci 42:453–459
4. Alexander KR, Barnes CS, Fishman GA (2003) ON-pathway dysfunction and timing properties of the flicker ERG in carriers of X-linked retinitis pigmentosa. Invest Ophthalmol Vis Sci 44:4017–4025
5. Barnes CS, Alexander KR, Fishman GA (2002) A distinctive form of congenital stationary night blindness with cone ON-pathway dysfunction. Ophthalmology 109:575–583
6. Dryja TP, McGee TL, Berson EL, Fishman GA, Sanberg MA, Alexander KR, Derlacki DJ, Rajagopalan AS (2005) Night blindness and abnormal cone electroretinogram ON responses in patients with mutations in the GRM6 gene encoding mGluR6. Proc Natl Acad Sci 102:4884–4889
7. Viswanathan S, Frishman LJ, Robson JG (2000) The uniform field and pattern ERG in macaques with experimental glaucoma: removal of spiking activity. Invest Ophthalmol Vis Sci 41:2797–2810
8. Kremers J, Lee BB, Pokorny J, Smith VC (1991) Linear analysis of macaque ganglion cell responses to complex temporal waveforms. Invest Ophthalmol Vis Sci Suppl 32:1090
9. Bush RA, Sieving PA (1996) Inner retinal contributions to the primate photopic fast flicker electroretinogram. J Opt Soc Am A 13:557–565
10. Alexander KR, Fishman GA, Peachey NS, Marchese AL, Tso MO (1992) 'On' response defect in paraneoplastic night blindness with cutaneous malignant melanoma. Invest Ophthalmol Vis Sci 33:477–483
11. Kondo M, Miyake Y (2000) Assessment of local cone on- and off-pathway function using multifocal ERG technique. Doc Ophthalmol 100:139–154
12. Chen C, Zuo C, Piao C, Miyake Y (2005) Recording rod ON and OFF responses in ERG and multifocal ERG. Doc Ophthalmol 111:73–81
13. Spekreijse H, van der Tweel H, Zuidema Th (1973) Contrast evoked responses in man. Vis Res 13:1577–1601
14. Riemslag FC, Ringo JL, Spekreijse H, Verduyn Lunel HF (1985) The luminance origin of the pattern electroretinogram in man. J Physiol 363:191–209
15. Bach M, Hoffmann M (2006) The origin of the pattern electroretinogram. In: Heckenlively JR, Arden GB (eds) Principles and practice of clinical electrophysiology of vision. MIT Press, Cambridge
16. Simpson M, Viswanathan S (2007) Comparison of uniform field and pattern electroretinograms of humans. J Mod Opt 54:1281–1288
17. Wässle H, Grünert U, Röhrenbeck J, Boycott BB (1989) Cortical magnification factor and the ganglion cell density of the primate retina. Nature 341:643–646
18. Wässle H, Grünert U, Röhrenbeck J, Boycott BB (1990) Retinal ganglion cell density and cortical magnification factor in the primate. Vis Res 30:1897–1991
19. Curcio CA, Sloan KR, Kalina RE, Hendrickson AE (1990) Human photoreceptor topography. J Comp Neurol 292:497–523
20. Curcio CA, Allen KA (1990) Topography of ganglion cells in human retina. J Comp Neurol 300:5–25
21. Sjöstrand J, Popovic Z, Conradi N, Marshall J (1999) Morphometric study of the displacement of retinal ganglion cells subserving cones within the human fovea. Graefes Arch Clin Exp Ophthalmol 237:1014–1023
22. Drasdo N, Fowler CW (1974) Non-linear projection of the retinal image in a wide-angle schematic eye. Br J Ophthalmol 58:709–714
23. Friedburg C, Allen CP, Mason PJ, Lamb TD (2004) Contribution of cone photoreceptors and post-receptoral mechanisms to the human photopic electroretinogram. J Physiol 556.3:819–834
24. Rangaswamy NV, Frishman LJ, Dorotheo EU, Schiffman JS, Bahrani HM, Tang RA (2004) Photopic ERGs in patients with optic neuropathies: comparison with primate ERGs after pharmacologic blockade of inner retina. Invest Ophthalmol Vis Sci 45:3827–3837
25. Ueno S, Kondo M, Ueno M, Miyata K, Terasaki H, Miyake Y (2006) Contribution of retinal neurons to d-wave of primate photopic electroretinograms. Vis Res 46:658–664
26. Viswanathan S, Frishman LJ, Robson JG, Harwerth RS, Smith EL III (1999) The photopic negative response of the macaque electroretinogram: reduction by experimental glaucoma. Invest Ophthalmol Vis Sci 40:1124–1136
27. Rangaswamy NV, Digby B, Harwerth RS, Frishman LJ (2005) Optimizing the spectral characteristics of a ganzfeld

stimulus used for eliciting the photopic negative response (PhNR). Invest Ophthalmol Vis Sci (Suppl) 46:4762

28. Holder GE (2001) Pattern electroretinography (PERG) and an integrated approach to visual pathway diagnosis. Prog Retin Eye Res 20:531–561

29. Kondo M, Miyake Y, Horiguchi M, Tanikawa A (1998) Recording multifocal electroretinogram on and off responses in humans. Invest Ophthalmol Vis Sci 39:574–580

30. Stiefelmeyer S, Neubauer AS, Berninger TA, Arden GB, Rudolph G (2004) The multifocal pattern electroretinogram in glaucoma. Vis Res 44:103–112

31. Klistorner AI, Graham SL, Martins A (2000) Multifocal pattern electroretinogram does not demonstrate localised field defects in glaucoma. Doc Ophthalmol 100:155–165

32. Harrison WW, Viswanathan S, Malinkovsky VE (2006) Multifocal pattern electroretinogram: cellular origins and clinical implications. Optom Vis Sci 83:473–485